▌**Dye Design** │*Hot Paper*│

Far-Red Emitting Fluorescent Dyes for Optical Nanoscopy: Fluorinated Silicon–Rhodamines (SiRF Dyes) and Phosphorylated Oxazines

Kirill Kolmakov,* Elke Hebisch, Thomas Wolfram, Lars A. Nordwig, Christian A. Wurm, Haisen Ta, Volker Westphal, Vladimir N. Belov,* and Stefan W. Hell*[a]

Abstract: Far-red emitting fluorescent dyes for optical microscopy, stimulated emission depletion (STED), and ground-state depletion (GSDIM) super-resolution microscopy are presented. Fluorinated silicon–rhodamines (SiRF dyes) and phosphorylated oxazines have absorption and emission maxima at about $\lambda \approx 660$ and 680 nm, respectively, possess high photostability, and large fluorescence quantum yields in water. A high-yielding synthetic path to introduce three aromatic fluorine atoms and unconventional conjugation/solubilization spacers into the scaffold of a silicon–rhodamine is described. The bathochromic shift in SiRF dyes is achieved without additional fused rings or double bonds. As a result, the molecular size and molecular mass stay quite small (< 600 Da). The use of the $\lambda = 800$ nm STED beam instead of the commonly used one at $\lambda = 750$–775 nm provides excellent imaging performance and suppresses re-excitation of SiRF and the oxazine dyes. The photophysical properties and immunofluorescence imaging performance of these new far-red emitting dyes (photobleaching, optical resolution, and switch-off behavior) are discussed in detail and compared with those of some well-established fluorophores with similar spectral properties.

Introduction

Near-IR emitting dyes are widely used in biology-related optical microscopy, modern super-resolution microscopy (e.g., stimulated emission depletion (STED) and ground-state depletion microscopy (GSDIM)), sensing, and materials science.[1] Red light is noninvasive, provides good tissue penetration depth, reduces scattering, and does not cause protein autofluorescence. It is also important that a variety of inexpensive, convenient, and powerful commercial lasers are available for this optical region (e.g., continuous-wave (CW) laser diodes, He—Ne, or krypton ion lasers). In STED microscopy, a laser beam selectively switches off the fluorescence of the molecules exposed to this depletion laser, so that the emitting area can be "squeezed" to a spot with dimensions no longer limited by diffraction.[2] Currently, a limited number of STED wavelengths are available in commercial STED microscopes: $\lambda = 592$–595, 660, and 765–775 nm.[3] Shifting the STED wavelength further to the near-IR spectral region is expected to cause less harm to biological objects and reduce photobleaching of the dye probe. As a result, with a STED beam of longer wavelengths ($\lambda > 775$ nm), better imaging performance can be achieved. However, STED microscopy with such a redshifted depletion beam has not been reported so far. Additionally, the redshift of the emission and absorption bands can expand the spectral window for dual and multicolor STED imaging schemes that utilize two or more dyes. Also, the bathochromic and bathofluoric shifts in some newly developed red-emitting dyes that are potentially applicable in living cells should require shifting of the STED wavelength as well. This would avoid the re-excitation of the dye fluorescence caused by the STED light.

New, efficient tools of dye design, "modular" approaches, and flexible synthetic routes to fluorophores with required spectral properties have been devised in recent years.[4] Due attention was paid to the solubility of the dyes in water, their net charge, and the hydrolytic stability of *N*-hydroxysuccinimidyl esters.[4,5] However, it still remains unclear how far one can shift the absorption and emission bands to the red spectral region, while still maintaining good performance under STED conditions and a sufficiently high fluorescence quantum yield (associated with the so-called brightness) of a dye. Rhodamine dyes based on a xanthene core with an oxygen atom at position 10 have found wide use as fluorophores due to their high photostability and large fluorescence quantum yields.[4,5] Our previous studies describe the synthesis, properties, and applications of red-emitting STED dyes with absorption and emission maxima at $\lambda = 635$–640 and 660 nm, respectively. To

[a] Dr. K. Kolmakov, E. Hebisch, Dr. T. Wolfram, L. A. Nordwig, Dr. C. A. Wurm, Dr. H. Ta, Dr. V. Westphal, Dr. V. N. Belov, Prof. S. W. Hell
Department of NanoBiophotonics
Max Planck Institute for Biophysical Chemistry
Am Fassberg 11, 37077 Göttingen (Germany)
E-mail: Kirill.Kolmakov@mpibpc.mpg.de
        vbelov@gwdg.de
        shell@gwdg.de

achieve these values, we used donor substituents at nitrogen atoms, additional double bonds and cycles, rigidized frameworks, and fluorinated phenyl rings at C-9.[5a–e] A further redshift for rhodamines is very difficult to achieve.[5g,6] An easier option to move to the IR region is to use carbopyronine dyes, in which the oxygen atom at position 10 of the xanthene fragment is replaced by a geminal dimethyl group (C(CH$_3$)$_2$).[7] This structural modification is known to cause a large bathochromic shift in the absorption and emission bands. Therefore, in this particular case (for carbopyronine dyes depleted by a $\lambda = 775$ nm STED laser), there is no need for four fluorine atoms in the o-substituted benzoic acid residue attached to C-9. One of the most practically important and commercially available carbopyronine dyes with a proven good performance in STED microscopy, ATTO 647N, absorbs at $\lambda = 644$ nm and emits at $\lambda = 669$ nm.[8] In general, the fluorine-free dyes are far less lipophilic, more soluble in aqueous buffers, possess high fluorescent quantum yields (even without additional polar groups), and perform well in STED microscopy.[5f] Unfortunately, the chemical structures of some commercially available red-emitting dyes remain undisclosed. The absence of these data complicates the proper choice of fluorescent dye for certain biochemical or imaging applications and hinders the design of new dyes. To create new photostable fluorophores for (multicolor) STED microscopy with variable STED wavelengths and to achieve further redshifts, new tools in dye design or new dye classes are required. A very efficient approach for a much larger bathochromic shift in xanthene dyes was reported in 2008.[9a] Thus, a family of silicon-containing rhodamines (known as SiR dyes or silarhodamines) was introduced.[9] They have a Si(CH$_3$)$_2$ residue (instead of oxygen) in position 10 of the (former) xanthene fragment, as seen in Scheme 1; and in this respect they are analogues of carbopyronines. The first striking feature of SiR dyes is a very large bathochromic and bathofluoric shift relative to conventional rhodamines (+ 90 nm) and carbopyronines (+ 45 nm). In particular, Si-TMR, which is the simplest N,N,N',N'-tetramethyl derivative of silicon–rhodamine, has an absorbance maximum at $\lambda = 645$–650 nm.[9b,h] 6-Carboxy-Si-TMR, which is usually called SiR-CO$_2$H or SiR for brevity, is a fluorogenic dye. Its monosubstituted derivatives exist in equilibrium between a nonfluorescent spirolactone ("OFF" state, closed form) and a fluorescent zwitterion ("ON" state, opened form; Scheme 1).[9h,k] Derivatives of SiR were successfully used for labeling SNAP-, CLIP-, and Halo-Tag fusion proteins in living cells.[9g,h,k,m] These and also actin and tubulin conjugates were successfully used in super-resolution imaging of living cells.[9g,h,k,m] In contrast, the SiR-methyl dye is nonfluorogenic (Scheme 1). A further redshift was not required for these dyes because STED was performed at $\lambda = 775$ nm.[9h,m] No additional methylene bridges or fused rings were attached to maintain a smaller molecular mass, size, and cell permeability. Notably, when the absorption and fluorescence maxima are shifted too far to the IR region ($\lambda > 700$ nm), the fluorescence quantum yield of dyes normally decreases.[9b] Therefore, the newly emerging dye candidates for STED microscopy should not have a very large bathochromic shift relative to those of well-established dyes (e.g., ATTO 647N, Abberior STAR RED or
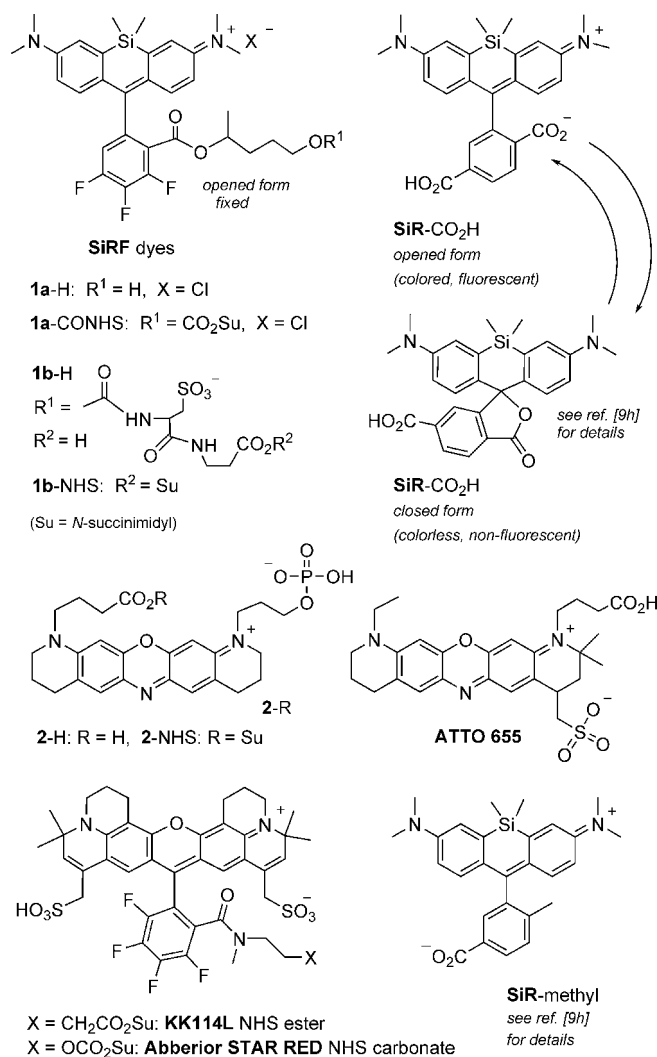
Scheme 1. Far-red emitting dyes: SiRF dyes (**1 a,b**), phosphorylated oxazine (**2**), and the reference red-emitting fluorescent dyes SiR-COOH (6-carboxy-Si-TMR), ATTO 655, KK 114L, Abberior STAR RED, and SiR-methyl. NHS = N-hydroxysuccinimide.

SiR-COOH) used with common STED wavelengths of $\lambda = 765$ and 775 nm.[3]

Results and Discussion

Motivation and general strategy

Pursuing our interest in exploring and optimizing new dyes for optical nanoscopy (STED and GSDIM[10]) in the far-red spectral region, we obtained and studied new silicon–rhodamines and oxazine dyes.[11] With regard to most biolabeling applications (conjugation) and imaging performance (brightness, photostability, absence of fluorescent background), additional properties of a dye are required. First, a versatile and generally applicable fluorescent marker needs to have a readily modifiable reactive group. If a dye can be decorated with a hydrolytically stable amino-reactive group, which allows prolonged storage in the solid state, then it can be easily transformed into other

↖↖ **These are not the final page numbers!**

reactive forms, such as azides and maleimides. In some cases, polar functional groups or additional solubilizing residues are highly desirable. They provide good solubility in water, increase the fluorescence quantum yield through disrupting aggregates, and reduce the undesired background caused by unspecific labeling. However, "compact" fluorophores with limited molecular mass (<800 Da) are most advantageous because they generally do not require additional polar groups for water solubility. The small size of the molecule is also beneficial for membrane permeability.[9h,k] It is known that the fluorescence quantum yield of a dye decreases dramatically if its absorption maximum lies beyond $\lambda = 700$ nm.[9b] Taking into account the spectral data of the simplest Si-TMR (absorption and emission maxima at $\lambda = 645$ and 661 nm, respectively; see Table 1),[9h] we decided to prepare related dyes with a moderate bathochromic shift. The introduction of several fluorine atoms into the phenyl ring attached to C-9 (meso position of the fluorophore) is one of the simplest ways to achieve a redshift in the xanthene scaffold.[5b,c,e] Multiple fluorine substituents in this phenyl ring are quite reactive towards nucleophiles,[5b,c] so it was a priori not clear if their presence was compatible with the multistep synthetic routes we had to follow. An additional redshift can be provided by amidation of the o-carboxyl group in the phenyl ring attached to the meso position (C-9) of the fluorophore.[5e] Rhodamines,[4,5] carbopyronines,[7] and silicon–rhodamines[9] usually have this group. Exceptions include the dyes SiR650, SiR680, SiR700, SiR720, and SiR-methyl,[9b,h] in which the carboxyl group is replaced by a methyl group, and an additional carboxyl group in the phenyl ring is used for conjugation. This approach blocks cyclization, but, on the other hand, does not provide an additional bathochromic shift. However, as a better and simpler solution, one can try amidation (or esterification) of the o-carboxyl group with a proper bifunctional substrate. That would fulfill all three tasks at the same reactive site of the dye: block cyclization into the non-fluorescent, closed, spirolactone form (see Scheme 1); provide a linker for conjugation through another reactive functional group at its terminus; and, additionally, produce a noticeable redshift. Additional double bonds or fused rings thus become unnecessary. Despite providing fluorogenicity,[9h,k] the ability of silicon–rhodamines to cyclize can be also a drawback: the colorless form might become dominating in the equilibrium inside a nonpolar medium. As a result, the fluorescent signal would drop dramatically. Generally, amidation or esterification of the sterically hindered o-carboxyl group represents a classical tool to create a spacer in dye chemistry. However, none of these reactions have been reported for silicon–rhodamine dyes so far.

Oxazine fluorescent dyes,[11] such as the dye ATTO 655 (Scheme 1),[8,12a] were shown to perform especially well in single-molecule localization microscopy.[10,12b] ATTO 655 has a sulfonic acid residue as a polar group, which provides good solubility in water. Highly polar dyes are known to have better fluorescence quantum yields in aqueous solutions and in conjugates as well. Also, they bind more specifically with the target structures, produce less background fluorescence, and yield bright and contrast-rich images with higher optical resolution.[5] Despite interesting spectral properties (Table 1), ATTO 655 has not yet found wide use in STED microscopy. As shown previously, phosphorylated rhodamines[5b–d] and coumarins[13a,b] could be even "brighter" dyes than the corresponding sulfonated analogues. The phosphonylation of cyanines, boron–dipyrromethene (BODIPY) fluorophores and perylenes was also used as a tool to prevent dye aggregation and improve the physicochemical properties.[13c–h] Therefore, another part of this research work focused on the synthesis of a new oxazine dye with a primary phosphate group (compound 2-H in Scheme 1) and its application in STED and GSDIM.

Table 1. Spectral properties of free SiRF dyes (**1a,b**-H, **15a**), phosphorylated oxazine **2**-H, and the reference dyes (SiR-methyl, SiR-CO₂H, ATTO 655, KK 114L, Abberior STAR RED), as well as related data for their conjugates with antibodies used for immunolabeling in STED and GSDIM.

Dye	Additional polar group	q[a]	Absorption[b] λ_{max} [nm]	Emission λ_{max} [nm]	$\varepsilon \times 10^{-5}$ [M⁻¹cm⁻¹]	Φ_{fl} [%][c]	τ [ns]	DOL[d]	Dye–antibody conjugates Φ_{fl} [%]	τ [ns]	STED:[l] resolution [nm], switch-off, re-excitation
1a-H	–	+1	662	680	1.18	66	2.4	2.3	35	2.4	63, +, –
1b-H	SO₃H	0	663	680	0.90	70	2.5	2.7	30	2.4	57, +, +
13a (13-O)[f]	–	+1	657	677	0.53[g]	63	–	–	–	–	–
15a	SCH₂CO₂H	−1	657	676	0.4	40	–	–	–	–	–
SiR-methyl	–	+1	648[h]	662[h]	1.0 h	39[h]	–	–	–	–	–
SiR-6-COOH	CO₂H	0	645[h]	661[h]	1.0[h]	39[h]	2.6	3.7	22	2.5	60, +, +++
2-H	OPO(OH)₂	−1	661	678	0.60	28	1.8	1.4	11	1.8	69, ++, +
ATTO 655	SO₃H	0	663	684	1.25[i]	30[i]	1.8[i]	0.8	12	1.8	65, ++, –
KK 114L	2×SO₃H	−1	637	660	0.92	55[i]	3.6	5.0	67	3.5	67, +++, +++
Abberior STAR RED	2×SO₃H	−1	636	659	1.0	66[k]	3.6	3.1	65	3.5	64, +++, ++

[a] Net charge in the conjugated state; for free dyes, this value is one unit lower. [b] All spectroscopic measurements for free dyes were recorded in water. [c] Determined for free dyes in solutions with the reference dye Atto AZ 237, unless otherwise stated. [d] DOL=degree of labeling; an average number of dye residues attached to one protein molecule with $M_r \approx 150\,000$ Da in sheep antimouse antibodies; see the Supporting Information for details. [e] Optical resolution (in nm), evaluation of the relative "switch-off" efficiency and relative re-excitation degree (see the main text for definitions, details, and discussion). [f] Because it did not have a conjugation site, dye intermediate **13a** was not used for immunolabeling (see Schemes 3 and 4 for the structure). [g] The lower extinction value was due to the equilibrium between the closed (colorless) and open (zwitterionic) forms in solutions of **13a**. [h] see ref. [9h]. [i] www.atto-tec.com. [j] See ref. [5c] and structure **2b** therein. [k] See ref. [5b], www.abberior.com and Scheme 1 for structures of the dyes. [l] With 800 nm light; see text for comparison of switch-off and re-excitation properties.
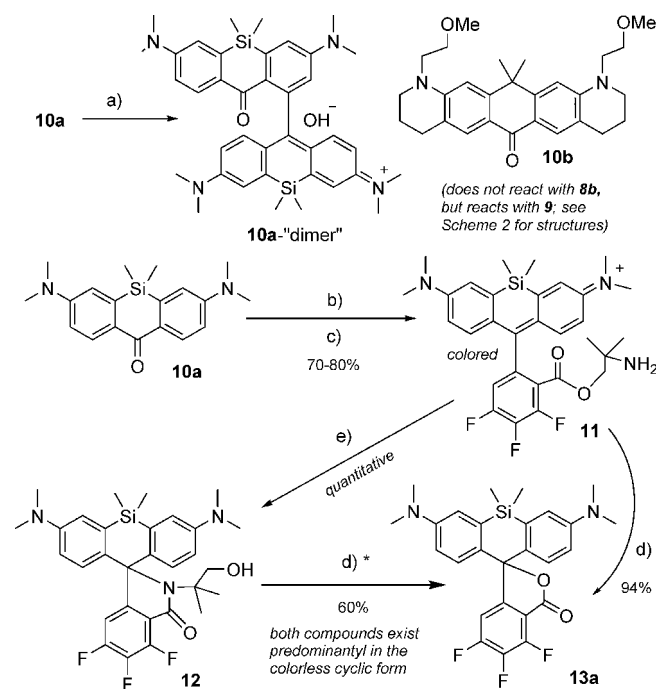
SiRF dyes

Initially, we tried to introduce four fluorine atoms into Si-TMR dye **1a** (Scheme 1) by using a known approach that worked well for non-fluorinated dye precursors. It was based on lithium–bromine exchange in 2-(2-bromophenyl)-4,4-dimethyl-2-oxazoline followed by reaction with the corresponding cyclic diaryl ketone.[5e] The chemistry related to the preparation of lithium reagents, starting from fluorine-substituted benzoic acids **3a,b**, is given in Scheme 2. We planned to use cyclic diaryl ketones (compounds **10a**[9c,h] and **10b**[5e] in Scheme 3) as
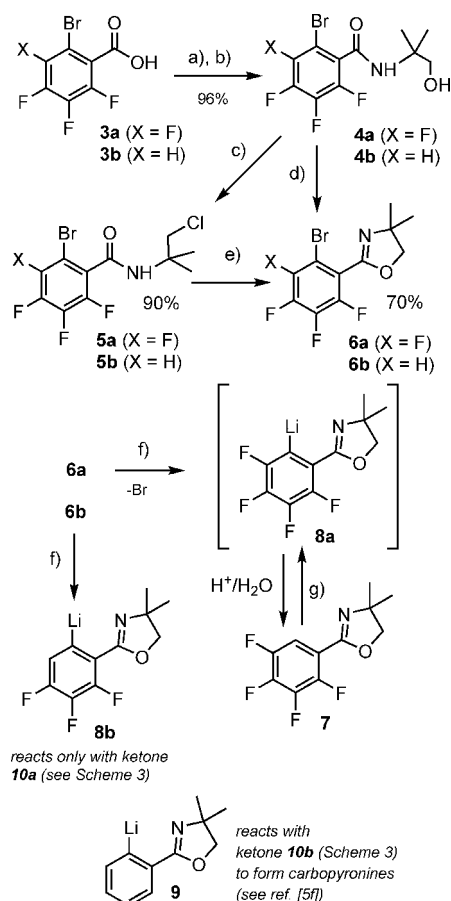
Scheme 2. Fluorinated oxazolines **6a,b** and their precursors: a) (COCl)$_2$, CH$_2$Cl$_2$, RT; b) 2-amino-2-methyl propanol, Et$_3$N, 0 °C; c) SOCl$_2$, RT; d) KHSO$_4$, 1,2-dichlorobenzene, 180 °C; e) *t*BuOK in THF or NaOAc in EtOH; f) *t*BuLi, THF, −78 °C; g) lithium 2,2',6,6'-tetramethylpiperidide (Li-TMP; prepared from 2.5 M *n*BuLi in hexanes and 2,2',6,6'-tetramethylpiperidine in THF), −78 °C to +5 °C.

the carbonyl substrates for further reactions with aryl lithium reagents. The starting amides **4a,b** with one bromine and three or four fluorine atoms in the aromatic ring were obtained with no difficulties (see the Supporting Information). However, the known cyclization assisted by thionyl chloride[9h] failed to convert amides **4a,b** into oxazolines **6a,b** (Scheme 2). Instead of oxazolines, ω-chloromethyl derivatives **5a,b** were formed. A base-induced cyclization of these undesired products caused substitution of fluorine (with *t*BuOK) or did not

work at all (with sodium acetate as a weaker base). Finally, we managed to perform the ring-closure reaction of amides **4a,b** to form oxazolines **6a,b** by using KHSO$_4$ (a moderately acidic heterogeneous dehydrating agent) in 1,2-dichlorobenzene at elevated temperatures. Disappointingly, all attempts to perform the required addition of *o*-lithiated oxazoline **8a** with four fluorine substituents (Scheme 2) to ketone **10a** (Scheme 3) failed. We established that *n*BuLi and *t*BuLi only

Scheme 3. Rhodamine lactone **13a** as the key building block for SiRF dyes: a) aryl oxazoline **7** (Scheme 2), Li-TMP, THF, hexane, −78 °C to RT; b) aryl oxazoline **6b** (Scheme 2), 1.5 M *t*BuLi in hexanes, THF, −78 °C; c) HOAc in MeOH, −10 °C; d) 20% aqueous HCl, 80 °C, 3 h; e) aq. NaHCO$_3$, RT. *: 30 h at 80 °C.

caused complete reductive debromination of oxazoline **6a**. Thus, after aqueous workup, bromine was lost (and compound **7** was isolated), but no further transformation occurred. However, the fact that all four fluorine atoms withstood the lithiation reaction was reassuring. This result indicated that the "benzine-type" intermediate with a triple bond had probably not been formed (because it would lead to the loss of a fluorine atom and a complex mixture of products) and ketone **10a** simply did not react with the quite stable lithiated oxazoline **8a**. An alternative synthetic pathway involved the lithiation of the corresponding "bromine-free" oxazoline **7** with Li-TMP followed by addition of ketone **10a** (Scheme 3).

This approach did not work either. Compound **7** and a new colored substance (**10a**-"dimer"; Scheme 3) were isolated from the reaction mixture. The formation of the dimer of ketone **10a** may be explained by the presence of a very strong base (excess Li-TMP was used). Li-TMP regioselectively deprotonates the aromatic ketone **10a** and the lithiated intermediate reacts with the keto group of another molecule. The intermediate lithiated ketone **10a** is stabilized by the keto group in the *o*-

↖↖ These are not the final page numbers!

position to the C–Li site. The dimer of compound **10a** has a brown color and also belongs to the silicon-rhodamine (SiR) dyes. The unexpected color (not blue!) indicates that the substituent at C-9 strongly influences the spectral properties of SiR dyes. An analogous lithiation of 3,4,5-trifluorobromobenzene with LiN(*i*Pr)$_2$ and the subsequent reaction of 2-lithio-3,4,5-trifluorobromobenzene with carbon dioxide were used for the preparation of 6-bromo-2,3,4-trifluorobenzoic acid (**3b**; Scheme 2).[14] Acid **3b** was used as a valuable intermediate to prepare oxazoline **6b** and check if its lithiated derivative (**8b** in Scheme 2) would react with cyclic diarylketones (**10a,b** in Scheme 3). The preparation of the building block **6b** involved amidation and cyclization steps (see the Supporting Information) and proceeded smoothly. Similarly, so did the one-pot reaction with the silicon-containing ketone substrate **10a** (see Scheme 3). The workup and product isolation were performed exactly as described for carbopyronine dyes[5f] to give the amino ester **11** (Scheme 3). The acidic deprotection of **11** gave the free silicon–rhodamine **13a**. This synthesis, as a whole, was straightforward and proceeded with high yields. Some important details are worth mentioning. First, one should avoid sodium bicarbonate and other bases during workup. Otherwise, the intermediate amino ester **11** rapidly undergoes cyclization into a very stable colorless spirolactame **12** (Scheme 3). This cyclization, which is clearly caused by an intramolecular nucleophilic attack, proved to be irreversible. Moreover, different to our previously explored carbopyronine spiroamide analogue,[5f] amide **12** is much more resistant to acidic hydrolysis (see the Supporting Information). Also, interestingly, polycyclic diaryl ketone **10b** did not react with *o*-lithiated oxazoline **8b**, but was known to react with compound **9** (Scheme 2).[5f] These observations support our assumption that *o*-lithiated oxazolines are readily formed and their reactivity increases in the following order: **8a** < **8b** < **9** (for structures, see Scheme 2). The very low reactivity of the polycyclic diaryl ketone **10b** (Scheme 3) can be explained by the inability of the amino groups to rotate. Their lone electron pairs are much better conjugated with

the keto group in compound **10b** than in ketone **10a**. As a result, the reactivity of **10b** towards nucleophiles (i.e., aryl lithium reagents) is reduced, compared with that of ketone **10a**, in which amino groups can rotate freely.

In the neat state and even in solutions (alcohols, DMF, MeCN), compound **13a** exists predominantly in its "closed" (colorless and nonfluorescent) lactone form (see Scheme 3, the relevant part of the Supporting Information, and photographs therein). It only develops a blue color in dilute aqueous solutions or when adsorbed on silica gel, as witnessed in the course of TLC or preparative column chromatography. With regard to spectral properties, the open form of SiRF **13a** (13-O$^-$ in Scheme 4) met our expectations. A sufficient bathochromic shift, relative to the previously studied red-emitting rhodamines and carbopyronine dyes (+20 nm; see Table 1),[5b–f] and to non-fluorinated SiR-CO$_2$H, was observed (+12 nm; Scheme 1).[9h] A relatively low extinction coefficient at the ab-
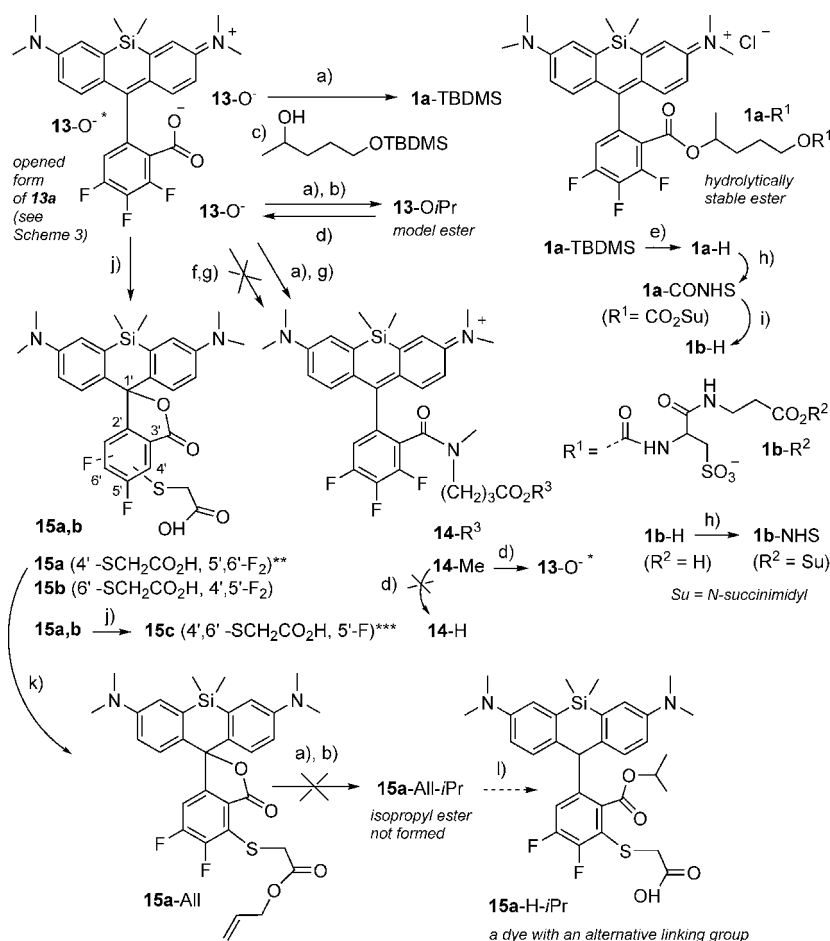
Scheme 4. Synthesis and transformations of SiRF dyes **1a,b**, which are fluorinated esters of silicon rhodamines: a) (COCl)$_2$, 1,2-dichloroethane, RT; b) propanol-2, RT; c) CH$_2$Cl$_2$, RT; d) 0.05 M NaOH in THF/H$_2$O (1:2), RT; e) aqueous HF in MeCN, RT; f) 2-(1*H*-7-azabenzotriazol-1-yl)-1,1,3,3-tetramethyluronium hexafluorophosphate (HATU), DMF; g) HCl·CH$_3$NH(CH$_2$)$_3$COOCH$_3$, Et$_3$N, CH$_2$Cl$_2$, DMF, RT; h) N,N'-disuccinimidyl carbonate (DSC), EtN*i*Pr$_2$, CH$_2$Cl$_2$, MeCN, RT; i) H$_3$N$^+$CH(CH$_2$SO$_3^-$)CONH(CH$_2$)$_2$CO$_2$H, Et$_3$N, HATU, DMF; j) HSCH$_2$CO$_2$H, Et$_3$N, MeCN, RT; k) allyl alcohol, N,N'-dicyclohexyl carbodiimide (DCC), Et$_3$N, 4-dimethylaminopyridine (DMAP); l) [Pd(Ph$_3$P)$_4$], HCOOH. *: the opened form of the silicon–rhodamine **13a** (see Scheme 3), which irreversibly forms the acid chloride upon treatment with (COCl)$_2$; **: the major isomer; ***: the disubstituted product is formed with an excess of HSCH$_2$CO$_2$H and/or at longer exposure times. TBDMS = *tert*-butyldimethylsilyl. For details of the syntheses and related analytical data, see the Supporting Information.

sorption maximum (53 000 $M^{-1}cm^{-1}$ at $\lambda=645$ nm in water; see Table 1) is clearly due to the equilibrium between the closed (**13a**) and opened forms (**13**-O⁻). The tendency of silicon–rhodamine **13**-O⁻ with three fluorine substituents (see Scheme 4) to cyclize into the colorless lactone form **13a** is so strong that it has to be accounted for during planning of its transformation into the "non-fluorogenic" and "fully colored" fluorescent dye. Thus, it was necessary to modify (block) the carboxylic group in such a way that it could no longer form the stable five-membered lactone ring. In particular, it proved impossible to perform aminolysis of lactone **13a** by using secondary aliphatic amines and HATU as a coupling reagent; this always worked well for rhodamine dyes.[5] The reason for this compound being unreactive is undoubtedly the presence of a base, which shifts the equilibrium fully to the closed form of **13a** (see Scheme 3 and Figure S2 in the Supporting Information). Thus, conversion to the corresponding acid chloride (**13**-Cl, R=Cl) was required.[15] Even less expected difficulty occurred when we converted compound **13a** into the acid chloride, attached the linker ($CH_3NH(CH_2)_3COOCH_3$ in Scheme 4), and isolated the amido ester **14**-Me. Although the amide bond is known to be quite stable toward hydrolysis over a wide range of pH, amide **14**-Me partly decomposed upon standing in a neutral organic solution at $+5\,°C$. Attempted saponification to the acid **14**-H, even with a very dilute aqueous alkali (0.05 M), immediately produced the starting rhodamine **13a** in its spirolactone form,[16] as observed by a complete loss of color. Therefore, we had to use an alternative type of a linker or reconsider the whole synthetic scheme to avoid a carboxyl group in the *ortho* position of the phenyl ring.

An ester group represents an alternative to the amide functionality. The hydrolytic stability of esters is generally far lower than that of amides, but it can be considerably improved by steric hindrance. As a simple model compound, we obtained the isopropyl ester **13**-O*i*Pr (from the acid chloride; see Scheme 4). Ester **13**-O*i*Pr demonstrated the required bathochromic shift and high quantum yield of fluorescence in water, despite the absence of polar groups (see Table 1). Fortunately, the compound proved sufficiently stable against weak bases (triethylamine in water). However, we established that the isopropyl ester **13**-O*i*Pr was cleaved within an hour, even with a 0.025 M solution of NaOH in water. Tertiary amines are involved as reagents in the preparation of *N*-hydroxysuccinimidyl esters or carbonates. The latter are more stable (yet react readily with primary amines)[5b] and their syntheses do not require the alkaline saponification of a methyl ester group attached to the linker. The risk of cleaving off the linker, as occurred with amide **14**-Me, was thus avoided. As a bifunctional linker, we chose a commercially available 1,4-pentanediol with the protected primary hydroxyl group. By using a large excess of the alcohol ($HOCH(CH_3)(CH_2)_3OTBDMS$), the ester **1a**-TBDMS was obtained in a high yield (Scheme 4). The cleavage of the TBDMS protecting group occurred partially during workup of the reaction mixture and was completed by a conventional method (dilute aqueous HF in MeCN).[17] The dye **1a**-H demonstrated sufficient solubility in water due to its CH_2OH group. The absorption and emission spectra were identical to those of

13-O*i*Pr (Table 1 and the Supporting Information) and the hydrolytic stability was even better. For the conjugation procedures, the amino-reactive form of a dye is required. Therefore, we prepared the NHS carbonate of **1a**-CONHS (Scheme 4). To this end, alcohol **1a**-H reacted with DSC in the presence of *i*Pr₂NEt as a base. Despite the expected partial cleavage of the linker in basic medium and the formation of the symmetrical carbonate, the amino-reactive marker **1a**-CONHS was obtained in moderate to good yields (up to 60%). Luckily, this product demonstrated very good hydrolytic stability and good reactivity towards amines. Importantly, in the test reactions with a large excess of dilute aqueous ammonia, triethylamine, and NaHCO₃, no cleavage of the linker was observed. Furthermore, bioconjugation reactions with antibodies proceeded with sufficient degrees of labeling (DOL), even though they were performed at relatively high pH values (8–8.5) in a NaHCO₃ buffer (see the Supporting Information). Also, being soluble in both water and nonpolar solvents, dye **1a**-H demonstrated amphiphilic properties, as seen in Figure S6 in the Supporting Information. To further improve dye **1a**-H by increasing its polarity and solubility in aqueous solutions, we attached a special solubilizing moiety—the so-called "universal hydrophylizer" ($H_3N^+CH(CH_2SO_3^-)CONH(CH_2)_2CO_2H$).[5a, 18] Such postsynthetic modifications, also introduced by Romieu and co-workers, were shown to drastically improve the solubility of dyes in water.[4l,m,r] Most importantly for immunolabeling, the polarity of dye residues prevents precipitation in the labeled proteins, reduces their "stickiness", unspecific binding, and the fluorescent background. As an overall result, the imaging performance of the hydrophilic dyes is often greatly improved. Thus, we subjected **1a**-CONHS to a reaction with a presynthesized peptide-like spacer that contained a sulfonic acid group (Scheme 4). As expected, the solubility of the reaction product **1b**-H in water became much better, while the fluorescence quantum yield in aqueous solutions increased (relative to the starting alcohol **1a**-H). The polar, free-dye **1b**-H proved to be quite stable in basic solutions (e.g., bicarbonate buffer and aqueous Et₃N), probably because of its zwitterionic character. The NHS ester of the modified dye **1b**-NHS demonstrated excellent hydrolytic stability and was isolated and handled in the pure state with no difficulties. Good hydrolytic stability of **1b**-NHS was in agreement with our previous observations on the stability of NHS ester dyes with a zero net charge: they were generally more stable than the negatively charged *N*-hydroxysuccinimidyl esters.[5b,c] Antibody staining with compound **1b**-NHS as a marker also proceeded with a high DOL.

An alternative way to modify the SiRF dyes was also explored. This involved aromatic nucleophilic substitution of the fluorine atom(s) with a thioglycolic acid residue (see Scheme 4). This approach was used, for example, in the synthesis of some red-emitting rhodamines and "masked" fluorescent dyes.[5a–c, 19] The silicon–rhodamine substrate **13a** (**13**-O⁻) did react with thioglycolic acid in the presence of triethyl amine. However, unlike tetrafluoro- or tetrachlorophenyl derivatives of xanthene dyes,[19] this reaction proved unselective. A 3:1 mixture of two regioisomers (**15a** and **15b**) was formed (see Scheme 4 and the Supporting Information for details). In

general, this derivatization method is potentially useful because compounds **15a** and **15b** are expected to be fluorogenic. These interesting dyes are difficult to separate (preparative HPLC is necessary). However, after isolation, each of them can be used as an analogue of SiR with slightly redshifted absorption and emission spectra. For example, 4-SCH$_2$COOH isomer **15a** (major product) has absorption and emission maxima at $\lambda = 657$ and 676 nm, respectively, a fluorescence quantum yield of 40%, and $\varepsilon \approx 40\,000$ (in water; see Table 1). The low ε value indicates that (even in aqueous solutions), compound **15a** exists mostly in the closed (colorless) form, in which one of the carboxylic groups is protected by the formation of a five-membered lactone ring. Organic solutions of both dyes **15a** and **15b** are nearly colorless. With this intrinsic protection, we first converted the SCH$_2$COOH group in **15a** into an allyl ester and then tried to transform another carboxyl group into an isopropyl ester by using the same methodology as that used for compound **13**-OiPr. Finally, we planned to cleave the allyl protective group and obtain a dye (**15a**-H-iPr) with a single, free carboxyl group available for conjugation (Scheme 4, bottom). However, the allyl ester (**15a**-All) formed neither the acid chloride nor the isopropyl ester (remained colorless), despite the large excess of oxalyl chloride. We can assume that a stable cyclic lactone ring remains intact under these reaction conditions. Additionally, we subjected the isopropyl ester (**13**-OiPr) to an S$_N$Ar reaction with triethylammonium thioglycolate under mild conditions. Disappointingly, this only led to the cleavage of the ester group, while the fluorine atoms remained unsubstituted (unlike in the case of "unprotected" rhodamine **13a**).

Phosphorylated oxazine dyes

Oxazines were shown to be very useful red-emitting fluorescent dyes.[11] In the design of dyes with tailored properties, it is always better to create a scaffold with multiple variable positions. We applied the oxazine-based scaffold of the kind (structure **20**-R^1,R^2) depicted in Scheme 5. Taking advantage of both variable positions in **20**-R^1,R^2, one can obtain dyes with variable net charges and functional groups. In this respect, the recently published results of Pauff and Miller were especially helpful because they enabled the creation of a general, most efficient, and high-yielding synthetic route to diverse oxazine dyes.[11b] Our optimized approach (Scheme 5) utilizes two key building blocks (**18** and **19**) obtained from a single precursor (compound **16**). Additionally, the hydroxyl group in the 3-hydroxypropyl residue offers further opportunities for modification of dyes.[5b,c, 16, 19b] In particular, it opens up an entry to fluorescent dyes with a primary phosphate group. The latter is very hydrophilic, polar, and brings a larger negative net charge than the conventional sulfonate. The presence of primary phosphate groups was shown to substantially improve the fluorescence quantum yields and solubility of rhodamines and coumarins in aqueous solutions.[5b–c, 13] The cationic oxazine dye **20**-Et,H demonstrated a sufficient bathochromic shift relative to most commonly used red-emitting rhodamines; it has absorption and emission maxima at $\lambda \approx 660$ and 676 nm, respec-
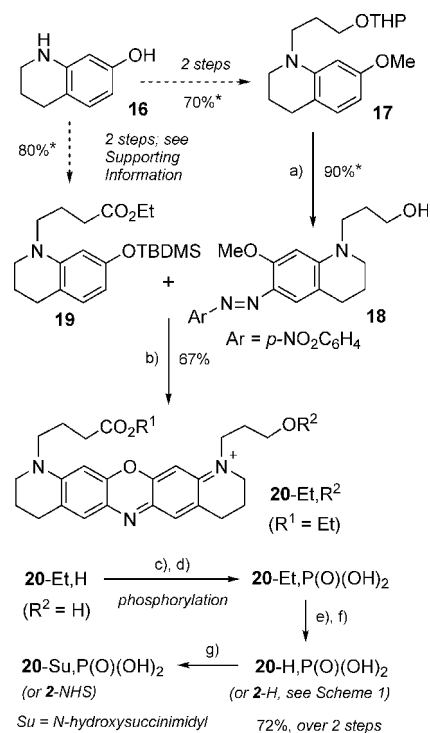
Scheme 5. Oxazine dyes with a primary phosphate group; condensation of the building blocks followed by phosphorylation: a) 4-O$_2$NC$_6$H$_4$N$_2$(+)·BF$_4$(−), dilute H$_2$SO$_4$ in aqueous MeOH, RT; b) 4 M HCl in EtOH, 85 °C; c) POCl$_3$, THF, 1,2-dichloroethane, 0 °C to RT; d) Et$_3$N, aqueous MeCN; e) 0.05 M aqueous NaOH; f) AcOH; g) N,N,N',N'-tetramethyl-O-(N-succinimidyl)uronium tetrafluoroborate (TSTU), Et$_3$N, DMF, RT. *: an average yield over two synthetic steps in 2–3 runs.

tively (Table 1). Ethyl ester **20**-Et,H was saponified with a dilute aqueous solution of NaOH and converted into the corresponding carboxylic acid **20**-H,H. Compounds **20**-Et,H and **20**-H,H are spectrally almost identical to the SiRF dyes described above (see the Supporting Information and Table 1 for the spectral data); only the solubility in water is very limited. In our preliminary experiments, the STED-imaging performance of dye **20**-H,H proved unsatisfactory. As usual, to obtain the antibody conjugates, carboxylic acid **20**-H,H was converted into the corresponding N-hydroxysuccinimidyl ester **20**-NHS,H (compounds **20**-H,H and **20**-NHS,H are not shown in Scheme 5). This drawback is because the single hydroxyl group, as a polar residue, is unable to prevent aggregation of the bulky and inherently hydrophobic oxazine molecules. To improve the dye brightness and overall imaging performance, we phosphorylated the alcohol **20**-Et,H by means of a straightforward procedure. As a reagent, we used POCl$_3$, and the intermediate phosphoric acid dichloride was hydrolyzed without purification (see the Supporting Information for details). As shown in Scheme 5, the phosphorylation of dye **20**-Et,H was followed by the saponification of ethyl ester **20**-Et,P(O)(OH)$_2$, which gave the free acid **20**-H,P(O)(OH)$_2$ (or **2**-H for brevity; see also Scheme 1). This dye demonstrated greatly improved imaging performance in STED and GSDIM (see Figures 1 and 4, below) relative to its non-phosphorylated precursor (**20**-H,H). As a proper reference dye for dye **2**-H, we chose ATTO 655 (see Scheme 1), which
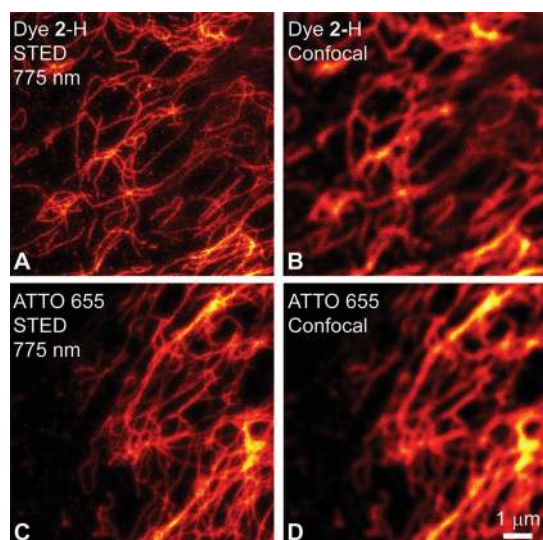
Figure 1. Far-red oxazine dyes in STED microscopy. STED and confocal images of the immunolabeled cytoskeletal protein vimentin in mammalian vero cells. The STED images were acquired by using excitation and depletion beams at $\lambda = 640$ and 775 nm, respectively. Confocal images of the same sample spot were acquired subsequent to the STED images by using an excitation beam at $\lambda = 640$ nm. A) Vimentin labeled with dye **2**-H; B) the corresponding confocal image of the same spot. C) Vimentin labeled with ATTO 655 dye; D) the corresponding confocal image (see the Supporting Information for details).

also belongs to the oxazine family. This comparison is reasonable because Atto 655 also has an anionic polar group, a sulfonic acid residue, which is the classical solubilizing moiety in dye chemistry. The spectral properties of ATTO 655 are almost identical to those of compound **2**-H (see Scheme 1 and Table 1). However, in STED microscopy (with a standard depletion laser of $\lambda = 775$ nm), dye **2**-H demonstrated a noticeable improvement over ATTO 655 (see Figure 1). Confocal images obtained with these dyes were indistinguishable. Both dyes have the same fluorophore and the only difference between them is that the phosphate group in **2**-H provides an additional negative net charge in conjugates ($q = -1$ at pH > 6). The overall polarity therefore appears much larger and this may result in better optical resolution and contrast, while the undesired background fluorescence is reduced (due to stronger repulsion of the dye residues from each other). These observations are consistent with our previous results on red-emitting rhodamine dyes with polar groups.[5b–f]

Spectral properties of SiRF dyes (1 a,b-H) and phosphorylated oxazine 2-H, and their performance in STED microscopy

Table 1 contains data on the spectral properties of free SiRF dyes (**1 a,b**-H, **15 a**), phosphorylated oxazine **2**-H, and reference dyes (SiR-methyl, SiR-CO$_2$H,[9h] ATTO 655,[8] KK 114L,[5c] Abberior STAR RED[5b]), as well as related data for their conjugates with antibodies applied in STED and GSDIM. As expected, due to the presence of three fluorine atoms and an ester group, compounds **1 a**-H and **1 b**-H demonstrated bathochromic and bathofluoric shifts (+ 14–17 nm and + 19 nm, respectively) in

comparison with the reference non-fluorinated dyes SiR-methyl and SiR-CO$_2$H.[9h] The positions of the absorption and emission maxima (as well as other parameters) were determined for aqueous solutions of dyes. All new dyes (**1 a**-H, **1 b**-H, and **2**-H) possess very similar spectral properties (Table 1). The absorption and emission maxima were found at $\lambda = 661$–663 and 678–680 nm, respectively. The Stokes shifts are relatively small (17 nm). Remarkably, the fluorescence quantum yields of SiRF dyes (**1 a,b**-H) in aqueous solutions are high (66 and 70%) and independent of the presence of polar groups (SO$_3$H in **1 b**-H). These values are higher than the fluorescence quantum yields of the reference dyes (SiR-methyl and SiR-CO$_2$H),[9h] compound **15 a**, both oxazines (**2**-H and ATTO 655[8]), as well as the benchmark polar dyes KK 114L[5c] and Abberior STAR RED.[5b] Solutions of the new and reference dyes (Table 1) in water and organic solvents (alcohols, acetonitrile, DMF, DMSO) are blue. (Compounds **15 a** and SiR-CO$_2$H give nearly colorless solutions in organic solvents.) The reference rhodamine dyes KK 114L and Abberior STAR RED show red fluorescence that is visible by the naked eye, whereas all other dyes emit invisible, near-IR light (see Figure S5 in the Supporting Information). Conjugates with antibodies were prepared according to the standard protocol. Moderate DOL values (0.8–2.7; Table 1) prevent aggregation and precipitation of the labeled proteins. Earlier we established that the STED imaging performance in the immunolabeled cell substrates weakly depended on the DOL values over quite a wide range.[5c,d] The fluorescence quantum yields of the conjugates varied from 11 to 35%. The highest values of Φ_{fl} in the conjugates (65–67%) were observed for highly hydrophilic and negatively charged rhodamine dyes (KK 114L and Abberior STAR Red) that possessed two sulfonic acid residues. However, even at the smallest values of Φ_{fl} (11–12%) for the oxazine dyes (ATTO 655 and **2**-H; Figure 1), it is possible to obtain good STED images. As expected, less hydrophilic and redshifted SiRF dyes demonstrated somewhat lower values of the fluorescence quantum yields in the conjugates: 22, 35, and 30% for SiR-CO$_2$H, **1 a-H**, and **1 b-H**, respectively. Remarkably, the fluorescence lifetimes of free dyes and their antibody conjugates were always constant (see Table 1). According to the values of the fluorescence lifetimes, all dyes can be separated into three distinct groups, which correspond to three dye classes: **1 a,b**-H and SiR-CO$_2$H (2.4–2.5 ns); **2**-H and Atto 655 (1.8 ns; the lowest value); KK 114L and Abberior STAR RED (3.8 ns; the highest value). These differences enable the fluorescence decay of two dyes to be registered separately,[20] and may even be three dyes (with very similar emission spectra), which present simultaneously as labels in a sample. Therefore, a set of two or three dyes from Table 1 can be applied in fluorescence lifetime imaging (FLIM). The new SiRF dyes (**1 a,b**-H) and phosphorylated oxazine **2**-H were compared with each other and the reference dyes (SiR-CO$_2$H,[9h] Atto 655,[8] KK 114L,[5c] Abberior STAR RED[5b]) in STED microscopy by using $\lambda = 640$ nm excitation and $\lambda = 800$ nm depletion beams.

The vimentin cytoskeleton was stained in mammalian cells by indirect immunofluorescence labeling with the dyes from Table 1 (Figure 2). The labeling protocols, sample preparation,
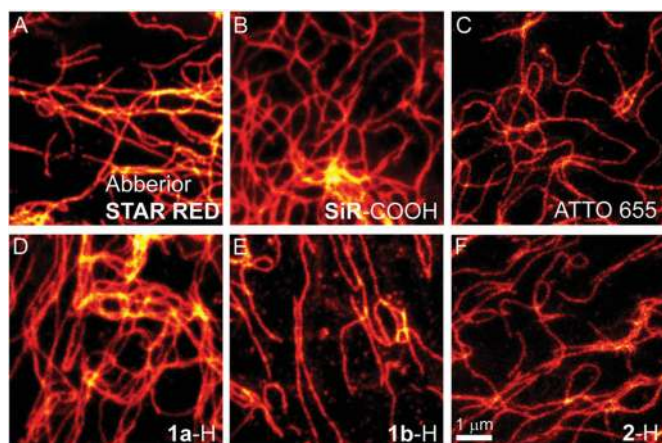
↖↖ These are not the final page numbers!

Figure 2. STED microscopy images of the immunolabeled cytoskeletal protein vimentin in mammalian cells. Images were acquired by using an excitation beam at $\lambda = 640$ nm and a depletion beam at $\lambda = 800$ nm for the dyes Abberior STAR RED, SiR-CO_2H, ATTO 655, **1a**-H, **1b**-H, and **2**-H. The images were taken according to the STED image acquisition procedure described in the main text and in the Supporting Information. For imaging performance parameters, see Table 1; for dye structures, see Scheme 1.

and preparation of the reactive markers (i.e., **1a**-CONHS, SiR-CONHS, **1b**-NHS, and **2b**-NHS) are described in Supporting Information.

The dyes ATTO 655, **1a**-H, **1b**-H, and **2**-H have an emission maximum at $\lambda \approx 680$ nm (redshifted by 20–25 nm relative to the most well-established near-IR emitting dyes), and therefore, better fit to a long-wavelength STED beam at $\lambda = 800$ nm. The applied power of the STED laser was 200 mW (at the back focal plane of the objective) at 80 MHz repetition rate (see the Supporting Information for more details). All new dyes enable us to obtain high-quality images by using redshifted excitation and depletion wavelengths ($\lambda = 640$ and 800 nm, respectively). This feature makes them especially valuable for staining biological samples because the near-IR STED light ($\lambda = 800$ nm instead of conventional $\lambda = 775$ nm) even further reduces the phototoxicity and enables deeper tissue penetration. The STED performance of dyes (as conjugates with antibodies) was evaluated and compared with respect to optical resolution, switch-off efficiency, and re-excitation by the very powerful $\lambda = 800$ nm light (Table 1). All dyes provided an optical resolution in the range of 57–69 nm (see the Supporting Information for the resolution determination details and an exemplary plot). The switch-off efficiency correlates with the ability of a dye to undergo the transition from the excited to the ground state when exposed to STED light. A better switch-off efficiency is thus expected to provide better optical resolution. The benchmark dyes KK 114L and Abberior STAR RED were only used up to now with $\lambda = 775$ nm STED laser, but they displayed the best switch-off ratios with $\lambda = 800$ nm STED light. Indeed, with $\lambda = 775$ nm STED light, these dyes were afforded the best optical resolution of 30–40 nm.[5c,d]

The oxazine dyes **2**-H and Atto 655 did not switch-off as readily as rhodamines KK 114L and Abberior STAR RED. The SiRF dyes **1a,b**-H, as well as SiR-CO_2H, switched-off even less efficiently than the oxazine dyes. The extent of re-excitation by

a STED beam represents another important parameter. Re-excitation is undesirable because it strongly compromises the image quality. The STED beam is usually strongly redshifted, even relative to the maximum of the emission band. Therefore, is not supposed to overlap with the absorption band of the dye. However, when the Stokes shift is small, a dye may have a residual absorption at the STED wavelength. In this case, a very strong STED pulse can excite the fluorescence of this dye to some extent. The STED beam may be represented as a doughnut (or other diffraction-limited pattern)[2b–d] with zero intensity only in the very center, so the fluorescence signal that originates in the course of re-excitation is "broad" (diffraction-limited) and registers as a relatively weak diffuse emission around the sharp elements of a STED image. The re-excitation phenomenon was not critical for these dyes, except probably compounds **1a**-H and ATTO 655. In this respect, it is worth mentioning that ATTO 655 is widely used in single-molecule studies, including photoactivated localization microscopy (PALM) and stochastic optical reconstruction microscopy (STORM; for additional references, see www.atto-tec.com),[12] but seldom in STED microscopy.[21] Dyes **1a,b**-H differ from the rest of the compounds in several respects (Table 1). Although they provide a lower switch-off ratio than other dyes, the optical resolutions observed with these dyes are the best (see the Supporting Information for resolution determination details). Second, they bear a positive (**1a**-H) or zero (**1b**-H and SiR-CO_2H) electric net charge on the dye residue in (bio)conjugates. Therefore, conjugates with small molecules (recognition units for the tagged proteins in living cells) are expected to be cell permeable. Further studies are necessary to clarify whether compounds **1a,b**-H represent viable markers for living cells. However, these new dyes (**1a,b**-H and SiR-CO_2H) turned out to be least photostable under STED conditions (Figure 3). The lower photostability of the silicon–rhodamines can be attributed to their nature: the tetramethyl silicon–rhodamine fluorophore is probably inherently less photostable than the oxazine core (**2**-H and ATTO 655) or the rigidized rhodamine fluorophore (KK 114L, Abberior STAR RED) additionally stabilized by the negatively charged polar residues.

Oxazine dyes 2-H and ATTO 655 in GSDIM

We decided to take a closer look at the performance of the oxazine dyes **2**-H and ATTO 655 (for structures, see Scheme 1) in GSDIM.[10,12b] We labeled nuclear pore complex subunits (in the central channel of the complex) by indirect immunofluorescence staining by using primary antibodies and secondary antibodies coupled with dyes **2**-H and ATTO 655. The labeled samples were mounted in GSDIM buffer with glucose oxidase (Glox) enzyme or in phosphate-buffered saline (PBS) solution (without additives of reducing agents) and observed in a GSDIM microscope (LEICA Microsystems). As seen in Figure 4, in GSDIM buffer, nanoscopy images can be generated by using the dyes Atto 655 and **2**-H. Importantly, in PBS solution, compound **2**-H provides much better images than those in Glox buffer. If we evaluate Figure 4C and D, we can see that compound **2**-H can be advantageously compared with dye ATTO
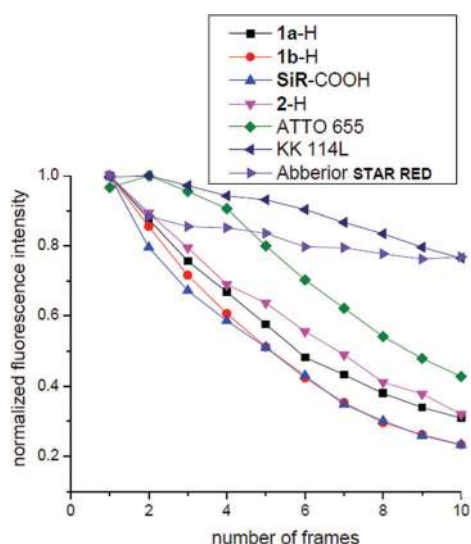
Figure 3. Bleaching behavior under STED conditions. Bleaching curves were obtained by using samples of the antibody-labeled protein vimentin in mammalian cells, as described in the Supporting Information. One sample spot was scanned 10 times by using both excitation and depletion beams at $\lambda = 640$ and 800 nm, respectively. Pixel intensities per frame were added and plotted against the number of frames. The resulting curves were normalized to their maximum value and plotted in one graph for comparison of the bleaching rates. For dye structures, see Scheme 1.
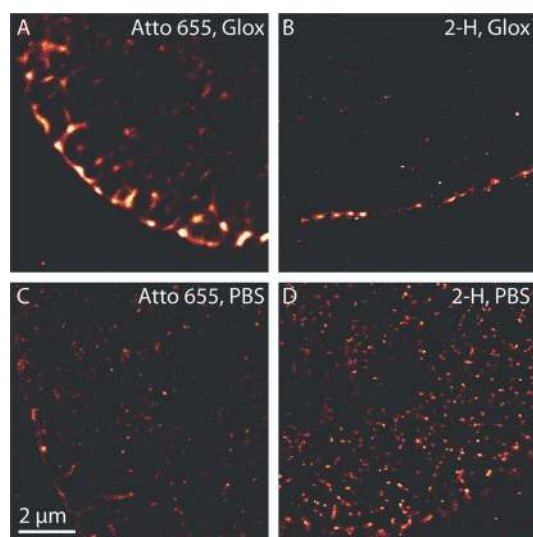

Figure 4. GSDIM images obtained with ATTO 655 and **2**-H dyes. Nuclear pore complexes of mammalian cells were labeled by indirect immunofluorescence with ATTO 655 (A, C) and **2**-H (B, D) dyes (see the Supporting Information for details). To compare the performance of the dyes in different buffers, the samples were then embedded in Glox/2-mercaptoethyl amine (MEA) buffer (A, B) and in PBS (C, D). Panels A) and B) contain images of the middle planes, whereas panels C) and D) represent images of the top planes of the nucleus. In both buffers, the average number of photons detected per event was about 450.

655: the image in Figure 4D is brighter, possesses better localization precision, and provides a more realistic (uniform) distribution of nuclear pore complexes (as confirmed by super-resolution STED microscopy). The good GSDIM performance of oxazine **2**-H in PBS is especially noteworthy because fluorophores

that show such properties in PBS are rare. Also, the presence of thiols in high concentrations or Glox may be prohibitive in the application of GSDIM to living cells.

Conclusion

Far-red emitting dyes are widely used in life sciences as fluorescent markers. The present study fully describes the synthesis and properties of SiRF dyes and phosphorylated oxazines with absorption and emission maxima at $\lambda \approx 660$ and 680 nm, respectively. In particular, a high-yielding synthetic pathway to introduce three "aromatic" fluorine atoms and additional conjugation/solubilization spacers into the scaffold of a silicon-containing tetramethylrhodamine (Si-TMR) and the related transformations are described in full detail. We introduced 2-(2-bromo-4,5,6-trifluorphenyl)-4,4-dimethyloxazoline (**6b**) as a new valuable building block for far-red emitting fluorophores. The bathochromic shift in the new Si-TMR derivatives is so large that it enables these dyes to be used in STED microscopy with $\lambda = 775$ or 800 nm depletion lasers (without additional structural modifications of the dyes, such as fused rings or extra double bonds). As a result, the size and molecular weight remain quite small (≈ 570 Da), which is very interesting in terms of cell permeability and the possibility of creating a "compact" fluorescent marker for lipids, carbohydrates, and other relatively small molecules. The new SiRF dyes are designed in such a way that cyclization to the colorless closed form is completely avoided. At the same time, both a bathochromic shift and conjugation linker are provided by proper modifications at the single reactive site of the silicon–rhodamine *o*-carboxyl group in the phenyl ring (attached to the C-9 *meso* position of the fluorophore). In these respects, SiRF dyes are alternatives to the dyes SiR680, SiR700, SiR720,[9b] and SiR-methyl.[9h] One should note that the equilibrium between the fluorescent open and nonfluorescent closed forms may appear as an undesired phenomenon. Some hydrophobic xanthene dyes with the "unprotected" *ortho*-carboxyl group may exist predominantly in the closed colorless form when the dye conjugate is placed into a nonpolar medium. In this regard, SiRF dyes are complimentary to fluorogenic silicon–rhodamines[9b,h,k] in which the very strong tendency to cyclize into the nonfluorescent lactone form is the main advantage. As we established, rhodamine carboxylic acid esters obtained from secondary alcohols could be good alternatives to classical amide-based spacers. Moreover, as a useful addition to the well-established dye SiR-CO₂H, we synthesized (presumably fluorogenic) compounds **15a,b** that contained the SCH₂COOH group as a second linking site. These bifunctional dyes were prepared by means of nucleophilic aromatic substitution (SNAr) of one fluorine atom in the SiRF dyes. In the solid state and in nonpolar media these compounds also exist predominantly in the closed colorless form. Therefore, their derivatives might be selective fluorescent markers for living cells. Importantly, these bifunctional dyes are spectrally redshifted by 10–12 nm relative to SiR-CO₂H (see Scheme 1 for structures).

Oxazine dyes also provide a sufficient redshift (absorption maximum at $\lambda = 660$ nm), yet the dye core is bulky and hydro-

↖↖ These are not the final page numbers!

phobic by nature. To improve the STED imaging performance of oxazine dyes, they were decorated with a phosphate group. The hydroxyl-containing dye substrate was subjected to a straightforward phosphorylation with $POCl_3$ in appropriate solvents (followed by hydrolysis in basic media). This simple phosphorylation protocol might be very useful in the long term because it completely avoids the formation of phosphonates (undesired side products; see ref. [13a]) and can be applied to a wide range of substrates with free hydroxyl alkyl groups. The phosphorylated zwitterionic dye (**2**-H) demonstrated high polarity, high solubility in water, and a negative net charge. It performed very well in GSDIM and demonstrated a greater improvement in STED images (especially with $\lambda = 755$ nm depletion laser) relative to its analogue ATTO 655.

A predictable and constant fluorescence lifetime (which does not change upon conjugation with various biological targets) is also a very important parameter of a fluorophore. If the fluorescence lifetimes of two or more spectrally similar emitters differ by about 0.6–0.8 ns, they can be detected separately by using a gated detector.[20] Oxazine dyes have not been used for such "lifetime separation" schemes so far, although they seem to have the shortest fluorescence lifetime among the microscopically useful fluorescent dyes. In the case of the oxazine dyes, the lifetime proves to be exactly the same (1.78–1.79 ns) with a very high precision for two different dyes in solution (dye **2**-H and Atto 655) and in their conjugates with different substrates as well. This remains true for other dyes such as silicon–rhodamines (dyes **1a**-H, **1b**-H, and SiR-CO$_2$H) and the "conventional" rhodamine KK114L (see Scheme 1 for structures). As a whole, we have a set of three lifetime values with noticeable differences: 1.8, 2.4, and 3.6 ns for oxazines, silicon–rhodamines, and conventional rhodamines, respectively (see also Table 1). If two detection channels (windows) for the "short" and "long" lifetimes are used, one can expect that oxazine and rhodamine dyes will be registered mainly in one channel (for the markers with short and long lifetimes, respectively), whereas silicon–rhodamines will appear in both channels significantly. This approach may help to discriminate between three markers by using only two detection channels.[23]

The photophysical properties and imaging performance of the new far-red emitting fluorophores are discussed in detail and compared with certain well-established "near-IR" dyes: SiR-CO$_2$H,[9h] ATTO 655 (see www.atto-tec.com), as well as benchmark dyes KK114L and Abberior STAR RED (www.abberior.com), although the last two dyes were designed for STED with $\lambda = 775$ nm laser.[22] This study has demonstrated that one can perform STED imaging with longer wavelength STED beams ($\lambda = 800$ nm) by using spectrally fitted far-red emitting dyes and the best near-IR rhodamine dyes. In the long term, the advantages of a red-shifted STED irradiation may become crucially important. Photodamage, protein autofluorescence, and light scattering would be reduced, while achieving deeper light penetration. The chemistry, scope, and applications of silicon–rhodamines and oxazines have been broadened and the great potential of these two important dye families has been shown.

[1] For reviews, see: a) M. Beija, C. A. M. Afonso, J. M. G. Martinho, *Chem. Soc. Rev.* **2009**, *38*, 2410–2433; b) E. M. S. Stennett, M. A. Ciuba, M. Levitus, *Chem. Soc. Rev.* **2014**, *43*, 1057–1075; c) M. Fernández-Suárez, A. Y. Ting, *Nat. Rev. Mol. Cell Biol.* **2008**, *9*, 929–943; d) M. S. T. Gonçalves, *Chem. Rev.* **2009**, *109*, 190–212; e) L. D. Lavis, R. T. Raines, *ACS Chem. Biol.* **2014**, *9*, 855–866; f) K. Umezawa, D. Citterio, K. Suzuki, *Anal. Sci.* **2014**, *30*, 327–349; g) S. van de Linde, M. Sauer, *Chem. Soc. Rev.* **2014**, *43*, 1076–1087; h) T. J. Chozinski, L. A. Gagnon, J. C. Vaughan, *FEBS Lett.* **2014**, *588*, 3603–3612; i) A. G. Godin, B. Lounis, L. Cognet, *Biophys. J.* **2014**, *107*, 1777–1784; for a recent report, see: j) J. B. Grimm, B. P. English, J. Chen, J. P. Slaughter, Z. Zhang, A. Revyakin, R. Patel, J. J. Macklin, D. Normanno, R. H. Singer, T. Lionnet, L. D. Lavis, *Nat. Methods* **2015**, *12*, 244–250.

[2] For background information and reviews, see: a) C. Eggeling, S. W. Hell, *STED Fluorescence Nanoscopy*, Springer Ser. in Fluorescence (Eds.: P. Tinnefeld, C. Eggeling, S. W. Hell), Springer, Berlin-Heidelberg, **2015**, p. 4–25; b) T. J. Gould, P. A. Pellett, J. Bewersdorf, *STED Microscopy. In: Fluorescence Microscopy: from Principles to Biological Applications*, **2013**, pp. 375–392, Wiley-VCH; c) D. A. Yushchenko, M. P. Bruchez, *Tailoring Fluorescent Labels for Far-Field Nanoscopy*, Springer Ser. in Fluorescence (Eds.: P. Tinnefeld, C. Eggeling, S. W. Hell), Springer, Berlin-Heidelberg, **2015**, p. 159–188.

[3] Leica Microsystems offers STED microscopes with $\lambda = 592$, 660, and 775 nm STED lasers; Abberior Instruments GmbH offers STED microscopes with $\lambda = 595$ or 775 nm STED lasers; Picoquant GmbH offers a STED microscope with a $\lambda = 765$ nm STED laser.

[4] For reviews on fluorescent dyes and most important achievements in this field, see: a) J. Lippincott-Schwartz, E. Snapp, A. Kenworthy, *Nat. Rev. Mol. Cell Biol.* **2001**, *2*, 444–456; b) D. S. Lidke, B. S. Wilson, *Trends Cell Biol.* **2009**, *19*, 566–574; c) G. Patterson, M. Davidson, S. Manley, J. Lippincott-Schwartz, *Annu. Rev. Phys. Chem.* **2010**, *61*, 345–364; d) E. Kim, S. B. Pak, Discovery of New Fluorescent Dyes: Targeted Synthesis or Combinatorial Approach. In *Advanced Fluorescence Reporters in Chemistry and Biology I: Fundamentals and Molecular Design* (Ed.: A. P. Demchenko), Springer, Berlin-Heidelberg, **2010**; e) *A Guide to Fluorescent Probes and Labeling Technologies*, Invitrogen, **2010** (11th Ed.), Carlsbad, USA; f) A. Romieu, D. Tavernier-Lohr, S. Pellet-Rostaing, M. Lemaire, P.-Y. Renard, *Tetrahedron Lett.* **2010**, *51*, 3304–3308; g) C. Petchprayoon, Y. L. Yan, S. Mao, G. Marriott, *Bioorg. Med. Chem.* **2011**, *19*, 1030–1040; for recent reports on rhodamines and related dyes, see: h) M. Sibrian-Vazquez, J. O. Escobedo, M. Lowry, F. R. Fronczek, R. M. Strongin, *J. Am. Chem. Soc.* **2012**, *134*, 10502–10508; i) A. Chevalier, P.-Y. Renard, A. Romieu, *Org. Lett.* **2014**, *16*, 3946–3949; j) C. Massif, S. Dautrey, A. Haefele, R. Ziessel, P.-Y. Renard, A. Romieu, *Org. Biomol. Chem.* **2012**, *10*, 4330–4336; k) A. Romieu, C. Massif, S. Rihn, G. Ulrich, R. Ziessel, P.-Y. Renard, *New J. Chem.* **2013**, *37*, 1016–1027; l) A. Chevalier, P.-Y. Renard, A. Romieu, *Chem. Eur. J.* **2014**, *20*, 8330–8337; m) A. Chevalier, K. Renault, F. Boschetti, P.-Y. Renard, A. Romieu, *Eur. J. Org. Chem.* **2015**, 152–165; n) E. Heyer, P. Lory, J. Leprince, M. Moreau, A. Romieu, M. Guardigli,

A. Roda, R. Ziessel, *Angew. Chem. Int. Ed.* **2015**, *54*, 2995–2999; *Angew. Chem.* **2015**, *127*, 3038–3042.

[5] For recent data on the chemistry and properties of rhodamine and carbopyronine dyes used in super-resolution optical microscopy, see: a) V. N. Belov, G. Yu. Mitronova, M. L. Bossi, V. P. Boyarskiy, E. Hebisch, C. Geisler, K. Kolmakov, C. A. Wurm, K. Willig, S. W. Hell, *Chem. Eur. J.* **2014**, *20*, 13162–13173; b) K. Kolmakov, C. A. Wurm, D. Meineke, F. Göttfert, V. P. Boyarskiy, V. N. Belov, S. W. Hell, *Chem. Eur. J.* **2014**, *20*, 146–157; c) K. Kolmakov, C. A. Wurm, R. Hennig, E. Rapp, S. Jakobs, V. N. Belov, S. W. Hell, *Chem. Eur. J.* **2012**, *18*, 12986–12998; d) C. A. Wurm, K. Kolmakov, F. Göttfert, H. Ta, M. L. Bossi, H. Schill, S. Berning, S. Jakobs, G. Donnert, V. N. Belov, S. W. Hell, *Optical Nanoscopy*, **2012**, *1*:7, DOI:10.1186/2192-2853-1-7; e) K. Kolmakov, V. N. Belov, J. Bierwagen, C. Ringemann, V. Müller, C. Eggeling, S. W. Hell, *Chem. Eur. J.* **2010**, *16*, 158–166; f) K. Kolmakov, V. N. Belov, C. A. Wurm, B. Harke, M. Leutenegger, C. Eggeling, S. W. Hell, *Eur. J. Org. Chem.* **2010**, 3593–3610; g) for the synthesis and properties of red-emitting rhodamines with extended π-conjugation systems, see: J. Liu, Z. Diwu, W.-Y. Leung, Y. Lu, B. Patch, R. P. Haugland, *Tetrahedron Lett.* **2003**, *44*, 4355–4359.

[6] Commercially available rhodamines 700 and 800 possess strong electron-accepting groups (CF_3 and CN) at the C-9 position. They absorb (emit) at $\lambda = 644$ ($\lambda = 664$) and 685 nm (710 nm), respectively. However, these dyes rapidly decolorize in neutral and basic aqueous solutions due to (reversible) addition of hydroxyl ions to C-9; see also: a) J. Arden-Jacob, *Neue langwellige Xanthen-Farbstoffe für Fluoreszenzsonden und Farbstofflaser* (Dissertation), Shaker Verlag GmbH, Aachen, Germany, **1993**; b) the structure of a rhodamine dye $CF^{TM}680R$ with absorption and emission maxima at $\lambda = 680$ and 701 nm, respectively, is unknown; see: www.linaris.de/php/CMS/usercontent/deutsch/PDFs/CF%20dye%20selection%20guide.pdf.

[7] For the basic chemistry and properties of carbopyronine dyes, see: a) C. Aaron, C. C. Baker, *J. Chem. Soc. B* **1971**, 319–324; b) J. Frantzeskos, *Neue langwellige Fluoreszenzfarbstoffe zur Markirung von Biomolekülen* (Dissertation), Shaker Verlag GmbH, Aachen, Germany, **2001**; c) J. Arden-Jacob, J. Frantzeskos, N. U. Kemnitzer, A. Zilles, K.-H. Drexhage, *Spectrochim. Acta Part A* **2001**, *57*, 2271–2283; d) R. O'Neill, P. V. Fischer (Guava Tech. Inc.), WO 2004/003510 (08. Jan. 2004); e) A. Zilles, J. Arden-Jacob, K.-H. Drexhage, N. U. Kemnitzer, M. Hammers-Schneider (Atto-Tec GmbH), WO 2005/003086 (13. Jan. 2005).

[8] For the properties of ATTO dyes, see: www.atto-tec.com. Other red-emitting dyes include ATTO 655 (oxazine) and (a new one; probably carbopyronine) ATTO 665. Both dyes absorb/emit with maxima at $\lambda = 663/684$ nm, but the fluorescence quantum yield of the former is 30%, and of the latter is 60% (all data were reported for aqueous solutions).

[9] For the synthesis, properties, and applications of silicon–rhodamines, see: a) M. Fu, Y. Xiao, X. Qian, D. Zhao, Y. Xu, *Chem. Commun.* **2008**, 1780–1782; b) Y. Koide, Y. Urano, K. Hanaoka, W. Piao, M. Kusakabe, N. Saito, T. Terai, T. Okabe, T. Nagano, *J. Am. Chem. Soc.* **2012**, *134*, 5029–5031; c) Y. Koide, Y. Urano, K. Hanaoka, T. Terai, T. Nagano, *ACS Chem. Biol.* **2011**, *6*, 600–608; d) T. E. McCann, N. Kosaka, Y. Koide, M. Mitsunaga, P. L. Choyke, T. Nagano, Y. Urano, H. Kobayashi, *Bioconjugate Chem.* **2011**, *22*, 2531–2538; e) T. Pastierik, P. Šebej, J. Medalová, P. Štacko, P. Klán, *J. Org. Chem.* **2014**, *79*, 3374–3382; f) P. Shieh, M. S. Siegrist, A. J. Cullen, C. R. Bertozzi, *Proc. Natl. Acad. Sci. USA* **2014**, *111*, 5456–5461; g) T. Wang, Q.-J. Zhao, H.-G. Hu, S.-C. Yu, X. Liu, L. Liu, Q.-Y. Wu, *Chem. Commun.* **2012**, *48*, 8781–8783; h) G. Lukinavičius, K. Umezawa, N. Olivier, A. Honigmann, G. Yang, T. Plass, V. Mueller, L. Reymond, I. R. Corrêa Jr, Z.-G. Luo, C. Schultz, E. A. Lemke, P. Heppenstall, C. Eggeling, S. Manley, K. Johnsson, *Nat. Chem.* **2013**, *5*, 132–139; i) E. Kim, K. S. Yang, R. J. Giedt, R. Weissleder, *Chem. Commun.* **2014**, *50*, 4504–4507; j) B. Wang, X. Chai, W. Zhu, T. Wang, Q. Wu, *Chem. Commun.* **2014**, *50*, 14374–14377; k) G. Lukinavičius, L. Reymond, E. D'Este, A. Masharina, F. Göttfert, H. Ta, A. Günther, M. Fournier, S. Rizzo, H. Waldmann, C. Blaukopf, C. Sommer, D. W. Gerlich, H.-D. Arndt, S. W. Hell, K. Johnsson, *Nat. Methods* **2014**, *11*, 731–733; l) P. Horváth, P. Šebej, T. Šolomek, P. Klán, *J. Org. Chem.* **2015**, *80*, 1299–1311; m) E. D'Este, D. Kamin, F. Göttfert, A. El-Hady, S. W. Hell, *Cell Reports* **2015**, *10*, 1246–1251; n) for a review, see: Y. Kushida, T. Nagano, K. Hanaoka, *Analyst* **2015**, *140*, 685–695.

[10] J. Fölling, M. L. Bossi, H. Bock, R. Medda, C. A. Wurm, B. Hein, S. Jakobs, C. Eggeling, S. W. Hell, *Nat. Methods* **2008**, *5*, 943–945. GSDIM: ground-state depletion followed by individual molecular return microscopy was performed by using a Leica SR GSD (3D) microscope. This super-resolution microscopy mode is based on the depletion of the fluorescent ("bright") state of all or nearly all molecules by shelving them in a dark (triplet) state. Subsequently, individual molecules return to the ground state (spontaneously or by triggering with UV light). These single markers have to be located at distances greater that the diffraction limit. They may be detected and localized by using a charge-coupled device (CCD) camera and collecting photons emitted by each of them. All of these events occur within micro- or milliseconds and can be repeated a hundred or thousand times. The acquisition of all of these "frames" enables the whole image to be reconstructed with a localization precision proportional to $1/\sqrt{\bar{N}}$.

[11] For the synthesis and properties of oxazine dyes, see: a) A. V. Anzalone, T. Y. Wang, Z. Chen, V. W. Cornish, *Angew. Chem.* **2013**, *125*, 650–654; b) S. M. Pauff, S. C. Miller, *Org. Lett.* **2011**, *13*, 6196–6199 (for the general synthetic scheme); c) A. Kanitz, H. Hartmann, *Eur. J. Org. Chem.* **1999**, 923–930; d) A. Zilles, J. Arden-Jacob, K.-H. Drexhage, N. U. Kemnitzer, M. Hamers-Schneider, US 2006/0179585A1; e) A. Toutchkine, WO 2009/152024A1; f) M. Hintersteiner, A. Enz, P. Frey, A. L. Jaton, W. Kinzy, R. Kneuer, U. Neumann, M. Rudin, M. Staufenbiel, M. Stoeckli, K. H. Wiederhold, H. U. Gremlich, *Nat. Biotechnol.* **2005**, *23*, 577–583; g) A. Wakata, H. M. Lee, P. Rommel, A. Toutchkine, M. Schmidt, D. S. Lawrence, *J. Am. Chem. Soc.* **2010**, *132*, 1578–1582; h) R. Herrmann, H. P. Josel, K.-H. Drexhage, N. J. Marx, EP 757447, 1996; i) U. Lieberwirth, J. Arden-Jacob, K.-H. Drexhage, D. P. Herten, R. Muller, M. Neumann, A. Schultz, S. Siebert, G. Sagner, S. Klingel, M. Sauer, J. Wolfrum, *Anal. Chem.* **1998**, *70*, 4771–4779; j) S. M. Pauff, S. C. Miller, *J. Org. Chem.* **2013**, *78*, 711–716.

[12] a) S. Wilmes, M. Staufenbiel, D. Lisse, C. P. Richter, O. Beutel, K. B. Busch, S. T. Hess, J. Piehler, *Angew. Chem. Int. Ed.* **2012**, *51*, 4868–4871; *Angew. Chem.* **2012**, *124*, 4952–4955; b) G. T. Dempsey, J. C. Vaughan, K. H. Chen, M. Bates, X. Zhuang, *Nat. Methods* **2011**, *8*, 1027–1036.

[13] a) S. Nizamov, K. Willig, M. Sednev, V. N. Belov, S. W. Hell, *Chem. Eur. J.* **2012**, *18*, 16339–16348; b) H. Schill, S. Nizamov, F. Bottanelli, J. Bierwagen, V. N. Belov, S. W. Hell, *Chem. Eur. J.* **2013**, *19*, 16556–16565; c) H. Hyun, H. Wada, K. Bao, J. Gravier, Y. Yadav, M. Laramie, M. Henary, J. V. Frangoni, H. S. Choi, *Angew. Chem. Int. Ed.* **2014**, *53*, 10668–10672; *Angew. Chem.* **2014**, *126*, 10844–10848; d) G. Battagliarin, M. Davies, S. Mackowiak, C. Li, K. Müllen, *ChemPhysChem* **2012**, *13*, 923–926; e) T. Bura, R. Ziessel, *Org. Lett.* **2011**, *13*, 3072–3075; f) F. Bruyneel, L. D'Auria, O. Payen, P. J. Courtoy, J. Marchand-Brynaert, *ChemBioChem* **2010**, *11*, 1451–1457; g) M. V. Reddington, *Bioconjugate Chem.* **2007**, *18*, 2178–2190; h) M. R. Mazières, C. Duprat, J. Bellan, J. G. Wolf, *Dyes Pigm.* **2007**, *74*, 404–409.

[14] E. Wallace, Y. H. Woon, J. P. Lyssikatos, WO2005051300A3, 15.09.2005.

[15] The reagents producing acid chlorides from rhodamines restrict the synthetic freedom. The sulfonic acid groups and other OH-containing moieties reactive towards oxalyl (thionyl)chloride or $POCl_3$ should be protected (or introduced in later synthetic steps). Otherwise sulfonic acids form sulfonyl chlorides that also react with amine substrates (that are usually used to attach conjugation linkers to the carboxyl sites).

[16] The instability of rhodamine amides towards alkaline hydrolysis has already been reported, see: V. P. Boyarskiy, V. N. Belov, R. Medda, B. Hein, M. Bossi, S. W. Hell, *Chem. Eur. J.* **2008**, *14*, 1784–1792.

[17] a) R. F. Newton, D. P. Reynolds, M. A. W. Finch, D. R. Kelly, S. M. Roberts, *Tetrahedron Lett.* **1979**, *20*, 3981–3982; b) E. M. Collington, H. Finch, I. J. Smith, *Tetrahedron Lett.* **1985**, *26*, 681–683.

[18] The details of preparation, properties, and the applicability of the "universal hydrophlilizer" will be reported later; for an example, see: Z. Diwu, Q. Meng, J. Liao, H. Guo, T. Dubrovsky, B. Abrams, PCT/US2011/044776.

[19] The aromatic nucleophilic substitution of fluorine or chlorine atom(s) in the tetrahalosubstituted *meso*-phenyl ring (attached to C-9) in xanthene dyes was studied by using thiols and amines as nucleophiles. This reaction is regioselective and leads to the products of (mono)substitution at C-6′ followed by substitution of the second halogen atom at C-5′, see: a) G. Yu. Mitronova, S. Polyakova, C. A. Wurm, K. Kolmakov, T. Wolfram, D. N. H. Meineke, V. N. Belov, M. John, S. W. Hell, *Eur. J. Org. Chem.* **2015**, 337–349; b) K. Kolmakov, C. Wurm, M. V. Sednev, M. L. Bossi, V. N. Belov, S. W. Hell, *Photochem. Photobiol. Sci.* **2012**, *11*, 522–532; c) Z. Diwu, J. Liu, R. P. Haugland, K. R. Gee, PCT WO 02/12195A1.

[20] F. Görlitz, P. Hoyer, H. J. Falk, L. Kastrup, J. Engelhardt, S. W. Hell, *Progr. In Electromagnetics Res.* **2014**, *147*, 57–84.

[21] For an example, see: http://www.activemotif.com/catalog/630/atto-sted-secondary-antibody-conjugates.

[22] The dye KK114L (previously reported as KK1119; see ref. [5d]) has the same fluorophore as KK114 (see refs. [5d, e], except the linker with a carboxylic acid residue is elongated by one CH_2 group. This provides a much more stable NHS ester (see ref. [5c]), although the spectral properties remain exactly the same. Abberior STAR RED (www.abberior.-com) is an NHS carbonate with the same fluorophore as that in KK114 (for the structure, see Scheme 1 and ref. [5d]). Under STED conditions, these two rhodamines are more photostable than SiR-CO_2H or SiRF

dyes, despite having additional conjugated double bonds (as seen in Scheme 1). The latter may undergo photoinduced reactions that cause partial bleaching (so-called "bluing", that is, hypsochromic and hypsofluoric shifts). No less importantly, derivatives of KK114 are far less sensitive to changes in the excitation/depletion conditions and other setup settings and develop far less re-excitation artifacts.

[23] A. Schönle, S. W. Hell, *Nat. Biotechnol.* **2007**, *25*, 1234–1235.

FULL PAPER

■ Dye Design

K. Kolmakov,* E. Hebisch, T. Wolfram,
L. A. Nordwig, C. A. Wurm, H. Ta,
V. Westphal, V. N. Belov,* S. W. Hell*

■■ – ■■

Far-Red Emitting Fluorescent Dyes for Optical Nanoscopy: Fluorinated Silicon–Rhodamines (SiRF Dyes) and Phosphorylated Oxazines

Edge of vision: Fluorinated silicon–rhodamines (SiRF dyes) and phosphorylated oxazines are applied in stimulated emission depletion (STED) and ground-state depletion microscopy (GSDIM) as new far-red-emitting fluorophores (see figure). Their photophysical properties and immunofluorescence imaging performance with a redshifted STED beam are discussed in detail and compared to those of some well-established near-IR emitting dyes.

↖↖ These are not the final page numbers!